An Impedance Approach to the Chiral Anomaly

Peter Cameron*
Strongarm Studios
Mattituck, NY USA 11952

(Dated: February 16, 2014)

Quantum impedances, both scale invariant and scale dependent, govern the flow of energy in quantum interactions. The chiral impedance is scale invariant, topological, can be identified with the vector Lorentz impedance of the quantum Hall effect. The traditional approach to the anomaly uses the fifth gamma matrix γ^5 to project out the chiral components, isolating the interaction of the wave function with the chiral potential from the overall dynamics. However, scale invariant impedances cannot couple energy, only communicate phase. A proper treatment requires consideration of the coupled dynamics of the full impedance network. Details of the calculation of π^0, η, and η' branching ratios via background independent quantum impedances are presented, followed by a brief discussion of the role of quantum impedances in the chiral anomaly, with an eye towards proton spin.

INTRODUCTION

In a finite quantum theory chiral symmetry is not broken. The anomaly seems to be an inevitable result of renormalization/regularization. However, one has a choice - in the presence of the anomaly *either* chiral symmetry *or* gauge invariance must be broken.

The requirement for gauge invariance is driven by the need to maintain phase coherence. Phase is relative. Quantum phase is not a single measurement observable. Yet quantum phase is deterministic in the projection operator, say in the single quantum measurements of amplitudes that comprise an interference pattern.

In the customary approach to gauge invariance, quantum phase coherence is maintained via the artifice of the covariant derivative. This is essential. A theory without quantum phase coherence is not a quantum theory.

The impedance approach is gauge invariant. Gauge invariance is built in. The scale invariant impedances - the far field photon impedance, the vector Lorentz impedance of both the quantum Hall effect and the QED chiral anomaly, the centrifugal impedance, the three-body impedance, the Coriolis impedance, and in general all impedances associated with inverse square potentials[1] - these impedances communicate both local and non-local quantum phase[2–4].

Complex impedances shift phases. Complex quantum impedances shift quantum phases. There is no need in the impedance approach for the artifice of the covariant derivative. One need only take the appropriate impedances into account.

The impedance approach is finite. Both the ultraviolet and the infrared divergences are removed by the impedance mismatches. Impedance is a geometric concept, depends on size and shape. In the limit of the small, the point/singularity is infinitely impedance mismatched to you and I. We cannot share energy with it. While equally decoupled, the quantum limit of the large is perhaps more subtle, in the realm of cosmology.

It follows that the chiral anomaly does not arise in the impedance approach. It is not unreasonable to expect that an approach which is both finite and gauge invariant would permit accurate calculation of the π^0 branching ratio[5–8], and much more.

QUANTUM IMPEDANCES

Every circuit designer knows - impedances govern the flow of energy. This is not a theoretical musing. Classical or quantum impedances, mechanical or electromagnetic, fermionic or bosonic, topological,... To understand the flow of energy it is essential to understand the relations between the relevant impedances.

A novel method for calculating mechanical impedances[9], both classical and quantum, was presented earlier[3]. In that work a background independent version of Mach's principle emerged from a rigorous analysis of the two body problem, permitting simple and direct calculation of these impedances.

The two body problem is innately one-dimensional. The mechanical impedances derived from Mach's principle can be converted to the more familiar electrical impedances by adding the attribute of line charge density, that of the the electric charge quantum confined to the Compton wavelength of the particle in question.

This method of generalizing quantum impedances from the photon and quantum Hall impedances to those associated with all potentials and forces provides a versatile tool, effectively applied to the elementary particle spectrum, the mechanics of local and non-local quantum state reduction, establishment of an exact relationship between gravity and electromagnetism, and a possible resolution of the black hole information paradox[3].

More recently, quantum impedances have been employed in exploring the role of time symmetry in quantum mechanics[4, 10], and the relationship of the impedance model to other interpretations of the formalism of quan-

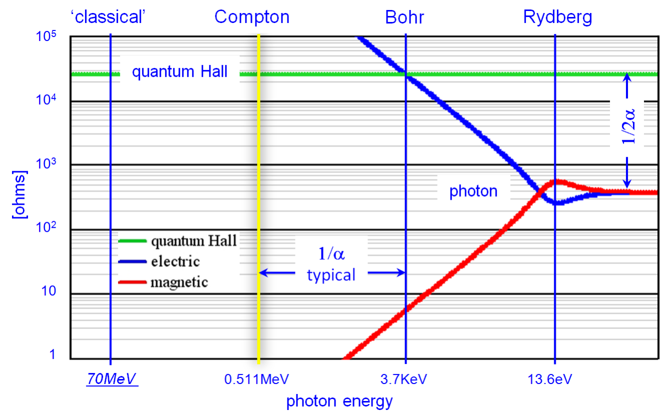

FIG. 1. Photon and electron impedances as a function of spatial scale as defined by photon energy. The role of the fine structure constant α is a prominent feature of the figure.

tum mechanics has been clarified[2].

In what follows the model upon which the impedance approach is based is briefly presented. Quantum impedance matching is then introduced via the Rosetta Stone of modern physics, the hydrogen atom.

The quantum impedance network and the unstable elementary particle spectrum are tied together by the manner in which the coherence lengths of the unstable particles are determined by the α-spaced conjunctions of the scale-dependent mode impedances. This is followed by application to branching ratio calculations of both the π^0 and the η, and a quantitative discussion of the η'.

THE IMPEDANCE MODEL

Physics without calculations is not physics, but rather philosophy. This novel tool, this method of calculating impedances, is of no use to physics without a model to which it may be applied. The model adopted earlier [3] remains useful. It comprises

- quantization of electric and magnetic flux, charge, and dipole moment
- interactions between these three topologies - flux quantum, monopole, and dipole
- confinement to a fundamental length, taken to be the Compton wavelength of the electron
- the photon

Coupling impedances of the interactions between these three topologies have been calculated[3, 12], and will be presented later in this note. With the exception of the impedances associated with inverse square potentials, they are parametric impedances, in the sense that they are scale dependent, and consequently energy dependent. As such, one might conjecture that they provide a confinement mechanism for the mode structures that are present in the impedance model.

THE HYDROGEN ATOM

The aim here is to see what insight into the hydrogen atom may be gained by exploring the role of quantum impedances in the transfer of energy from a 13.6eV photon to an electron.

In figure 1 the scale invariant far field photon impedance is the red line entering the plot from the right at Z_0 ~377 ohms. The photon impedance is strictly electromagnetic. Unlike massive particles, it has no mechanical impedance. Also shown in the figure is the scale invariant quantum Hall impedance, at R_H ~25.8 Kohm. It is an electromechanical impedance.

The wavelength of the 13.6eV photon is the inverse Rydberg. The electric and magnetic flux quanta that comprise a photon of that energy decouple there, at the transition from the scale invariant far field to the scale dependent near field[11]. The decoupled flux quanta are not scale invariant, electric going to high impedance and magnetic to low as one moves to shorter length scales.

The far field photon is mismatched to the electron quantum Hall impedance. The electric component of the photon near field dipole impedance does indeed match the quantum Hall impedance at the Bohr radius. However, for energy to flow smoothly and continuously from the photon to the electron, from the Rydberg to the Bohr radius, requires a smooth and continuous match to an electron dipole impedance, a quantum dipole impedance.

While such an impedance is not to be found in the canonical literature, it exists in the impedance model, and is shown in the impedance plot of figure 2. The electric flux quantum is well matched to the larger of the two electric dipole impedances of the electron, the 'external' dipole impedance, where the electric dipole impedances are represented by large and small blue diamonds.

The impedance plot of figure 2 was generated with the electron in mind, with no thought of the hydrogen atom or the photon. It was only later that the photon was added. The resulting smooth impedance match from the photon at the Rydberg to the electron at the Bohr radius and the consequent 'Bohr correspondence' was a nice serendipitous surprise.

As the head of the **electric flux quantum** wavepacket arrives at the Bohr radius the (presumed Gaussian) packet is still feeding increasing energy in from out beyond the Rydberg. From figure 2 it can be seen that at the Bohr radius there is a conjunction (upper dashed circle) of the electron dipole impedance with the scale invariant electric and magnetic vector Lorentz impedances, the scale invariant centrifugal impedance, and the scale dependent electric Coulomb and scalar

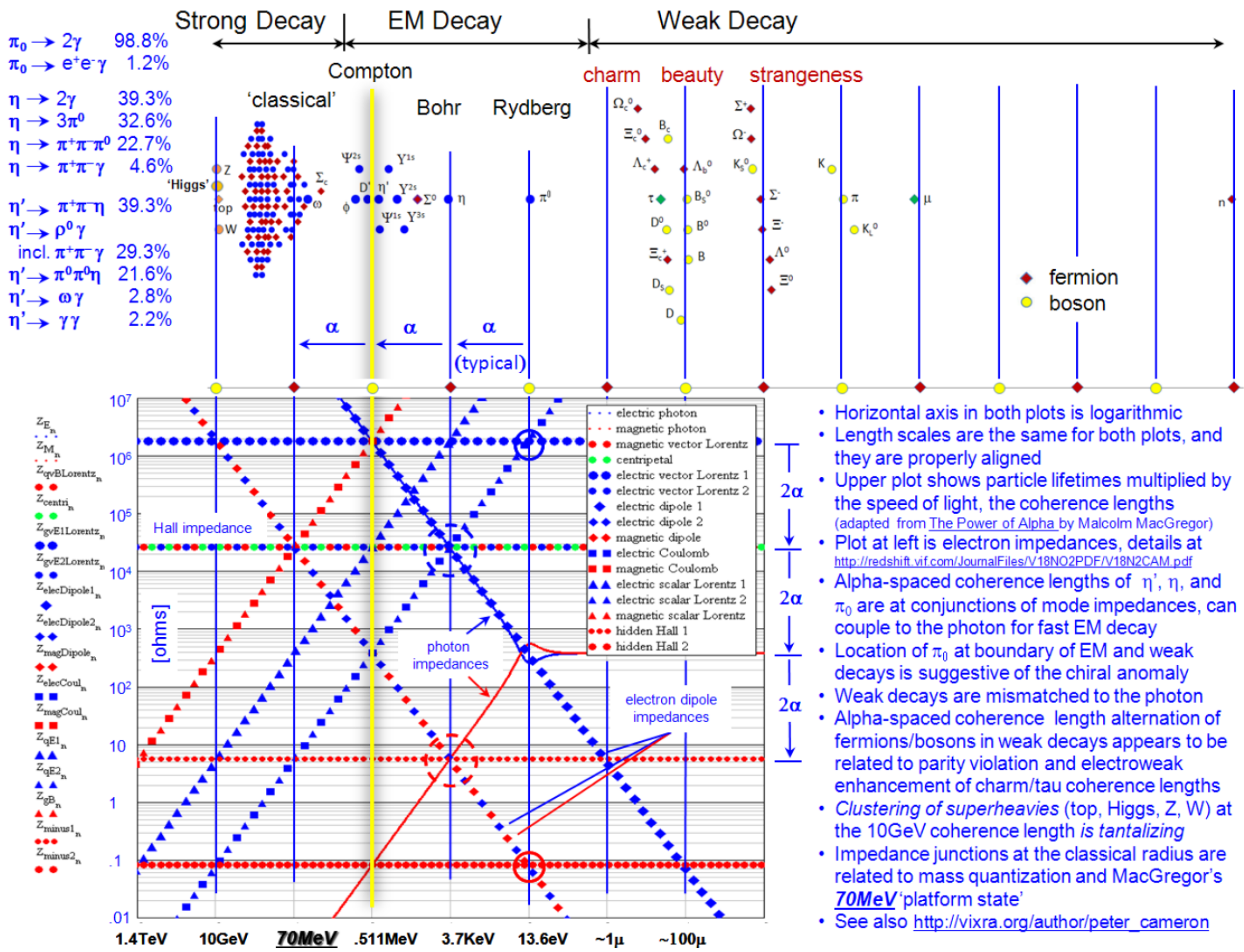

FIG. 2. A composite of 13.6eV photon impedances and a variety of background independent electron impedances[12], measured branching ratios of the π^0, η, and η', the four fundamental quantum lengths shown in fig.1, and the coherence lengths of the unstable particles.[13–15]

Lorentz impedances. The details of the couplings between the modes associated with the impedances (phases, confinement mechanisms,...) remain to be investigated. At the outset it is tempting to say that one knows the outcome (the H atom is ionized) and can work backwards from there.

But where is the proton in this plot? Given that the many many short-lived resonances between the 70MeV classical radius and the 9.59GeV coherence line are adequately represented by the subset shown (more on the neutrino later), only the proton is absent. What is it that the electron is ionized from by that 13.6eV photon? The plot is in the rest frame of the electron.

The **magnetic flux quantum**, unlike the electric flux quantum, arrives at the Bohr radius without benefit of an impedance match from the scale of the Rydberg, but presumably still phase-coherent. The excitation of the Bohr magneton (an 'internal impedance' denoted by the small red diamonds) at the Bohr radius is more of a shock excitation, more broadband.

The possible existence of at least one scale invariant magnetic impedance should be noted, present at the five ohm conjunction (lower dashed circle) of the magnetic flux quantum with the magnetic and the smaller of the two electric dipole impedances. Detailed calculations suggest that the measured quantum Hall impedance is not just an electric impedance, but rather the sum of the scale invariant electric *and* magnetic impedances.

It was shown earlier[3] that all massive particles have an inertial impedance, a centrifugal impedance, represented by the green dots in figure 2. Similar to the case of additional scale invariant magnetic impedances, one might consider the existence of the corresponding additional scale invariant centrifugal impedances, and perhaps the full family of invariant impedances associated with the inverse square potentials.

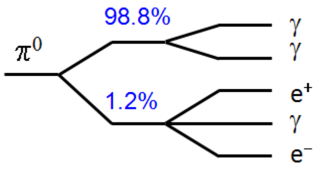

FIG. 3. The π^0 branching tree

THE π^0 BRANCHING RATIOS

The relatively simple π^0 branching tree is shown in figure 3. As the image suggests, the impedance calculation is done taking the paths in parallel.

As shown in figure 2, the π^0 coherence length coincides with the (inverse) Rydberg, where there is an impedance match via the dipole mode. Ignoring the phases, the impedance of the two photon mode can be written as

$$Z_{\gamma\gamma} = \frac{1}{\frac{1}{Z_0} + \frac{1}{Z_0}} = 188.37\,\Omega \tag{1}$$

and that of the e$^+$e$^-$$\gamma$ mode as

$$Z_{ee\gamma} = \frac{1}{\frac{1}{R_H} + \frac{1}{R_H} + \frac{4\alpha^2}{Z_0}} = 12\,813\,\Omega \tag{2}$$

where $R_H = \frac{Z_0}{2\alpha}$ is the quantum Hall resistance, so that

$$Z_{\pi 0} = \frac{1}{\frac{1}{Z_{\gamma\gamma}} + \frac{1}{Z_{ee\gamma}}} = 185.64\,\Omega \tag{3}$$

and the branching ratios are

$$\Gamma_{\gamma\gamma} = \frac{Z_{\pi 0}}{Z_{\gamma\gamma}} = 0.9855 \tag{4}$$

$$\Gamma_{ee\gamma} = \frac{Z_{\pi 0}}{Z_{ee\gamma}} = 0.0145 \tag{5}$$

These branching ratios are in agreement with the measured values shown in figures 2 and 3 at slightly better than three parts per thousand, suggesting that higher order corrections go as powers of $\sim\frac{\alpha}{\pi}$.

THE η BRANCHING RATIOS

The more complex η branching tree is shown in figure 4. Here we follow the same method as in the previous example, working from right to left in the figure as we calculate. Again ignoring the phases, as well as factors of two that will be addressed in the discussion that follows, the impedance of the two photon mode can be written as

$$Z_{\gamma\gamma} = \frac{1}{\frac{2}{Z_0} + \frac{2}{Z_0}} = 94.183\,\Omega \tag{6}$$

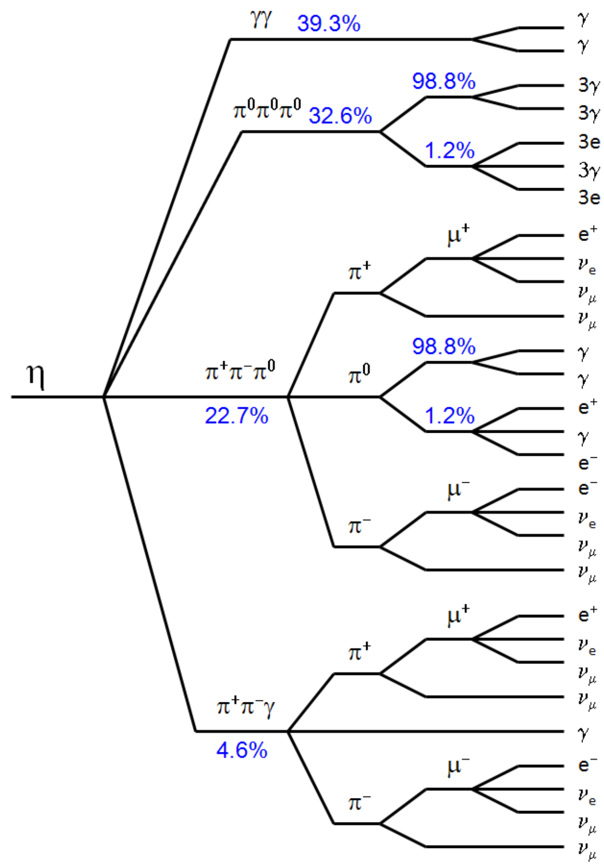

FIG. 4. The η branching tree

The π^0 impedance calculated in the previous section is used to find that of the three π^0 mode

$$Z_{3\pi 0} = \frac{2}{\frac{1}{Z_{\pi 0}} + \frac{1}{Z_{\pi 0}} + \frac{1}{Z_{\pi 0}}} = 123.76\,\Omega \tag{7}$$

The impedance of the $\pi^+\pi^-\pi^0$ mode is

$$Z_{\pi\pi\pi 0} = \frac{1}{\frac{1}{Z_{\pi+}} + \frac{1}{Z_{\pi-}} + \frac{1}{Z_{\pi 0}}} = 175.54\,\Omega \tag{8}$$

where we assume the neutrino has rest mass, and therefore a scale invariant centrifugal/quantum Hall impedance

$$Z_\nu = R_H = 25\,812.8\,\Omega \tag{9}$$

so that the muon impedance is

$$Z_\mu = \frac{R_H}{3} = 8\,604.3\,\Omega \tag{10}$$

The impedances of the charged pions are then

$$Z_{\pi+} = Z_{\pi-} = \frac{1}{\frac{1}{Z_\nu} + \frac{1}{Z_\mu}} = 6\,453.2\,\Omega \tag{11}$$

And finally the impedance of the $\pi^+\pi^-\gamma$ mode is

$$Z_{\pi\pi\gamma} = \frac{2}{\frac{1}{Z_{\pi+}} + \frac{1}{Z_{\pi-}} + \frac{1}{Z_0}} = 674.69\,\Omega \quad (12)$$

so that the impedance of the η is

$$Z_\eta = \frac{2}{\frac{1}{Z_0} + \frac{1}{Z_{3\pi0}} + \frac{1}{Z_{\pi\pi\pi0}} + \frac{1}{Z_{\pi\pi\gamma}}} = 38.644\,\Omega \quad (13)$$

and the branching ratios are

$$\Gamma_{\gamma\gamma} = \frac{Z_\eta}{Z_{\gamma\gamma}} = 0.410 \quad (14)$$

$$\Gamma_{3\pi0} = \frac{Z_\eta}{Z_{3\pi0}} = 0.312 \quad (15)$$

$$\Gamma_{\pi\pi\pi0} = \frac{Z_\eta}{Z_{\pi\pi\pi0}} = 0.220 \quad (16)$$

$$\Gamma_{\pi\pi\gamma} = \frac{Z_\eta}{Z_{\pi\pi\gamma}} = 0.057 \quad (17)$$

As can be seen from figure 4 (or the corresponding modes of figure 5, for that matter), all four branching ratios are in agreement with the measured values at better than two parts per hundred.

THE η' BRANCHING RATIOS

The η' branching tree is shown in figure 5. Unsurprisingly, following the same method as in the previous examples gives reasonable results for some but not all branches. Looking at figure 2, it's not hard to see why.

The π^0 coherence length sits at the inverse Rydberg, well isolated from perturbation due to either the η at smaller length scales or τ and the charm family at greater scales. Similarly, the η stands on its own at the Bohr radius, with the Σ^0 nearest neighbor.

Unlike the π^0 and η, the η' is in the thick of it, with its coherence length at the Compton wavelength of the electron, right in the middle of the mode structure of the excited flavor states. It seems most probable that coupling to those states (and perhaps other effects resulting from the fact that in the impedance model the electron Compton wavelength is taken to define a fundamental length, the quantization scale) will require a more sophisticated treatment than that given the π^0 and η.

Again looking at figure 2, it remains that the similarity of the impedance structures at the Bohr radius and the Compton wavelength likely accounts for the similarity in the values of the relative branching ratios of the η and η' tabulated in the upper left corner of the figure. The measured branching ratios of the largest mode are equal, and the rest agree within a couple percent. Just the players are different. The ratios are pretty much the same, determined by the similar impedance structures.

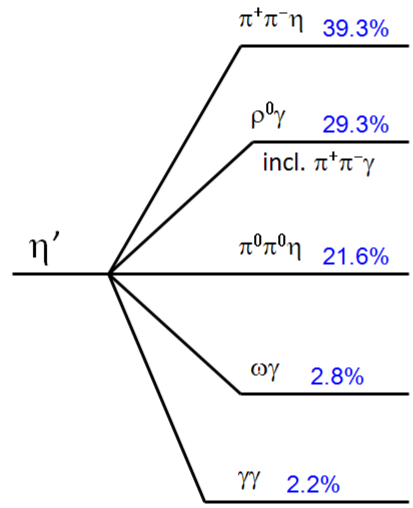

FIG. 5. The η' branching tree

FACTORS OF TWO

Unexplained factors of two are present in the impedance model. The first, and most bothersome, is in the definition of the quantum Hall resistance,

$$R_H = \frac{Z_0}{2\alpha} \quad (18)$$

That factor of two is present in the vertical scale of figures 1 and 2, but absent from the horizontal scale. Yep. I jiggered the horizontal scale. If one looks at the mathcad file that generates the figures[12], it becomes apparent. While the Compton radius is where it belongs, according to the calculations the impedance conjunctions associated with the 'classical' radius should be not at

$$r_{classical} = \alpha\lambda_{Compton} \quad (19)$$

but rather a factor of two closer, at

$$r_{junction} = \frac{\alpha}{2}\lambda_{Compton} \quad (20)$$

Similarly, the conjunctions at the Bohr radius are a factor of two closer to the Compton wavelength, those at the Rydberg a factor of four,... A simple solution could be to take $R_H = \frac{Z_0}{\alpha}$ rather than $R_H = \frac{Z_0}{2\alpha}$. At the time that seemed like a radical step.

Factor of two offsets are also present in the scale dependent impedances, and in the corresponding work of MacGregor[15] as well. As mentioned earlier[3], without understanding how to properly attribute them (after all, the impedance model is yet in its infancy) and in the interest of simplicity, they were kept in mind but eliminated from the model until such time as they were in need of attention. They will likely be of help in untangling the mode structures, in exploring connections between impedances and say quarks and gluons,...

	'spinor' **flux quantum**	monopole **charge quantum**	dipole **dipole quantum**
electric	dark	observable	dark
magnetic	observable	dark	observable

FIG. 6. Alternation of dark and observable with topology

DISCUSSION

The impedance plot of figure 2 is not complete. *Absent* are the longitudinal dipole-dipole impedances, the longitudinal and transverse charge-dipole impedances (the charge-dipole impedances are scale invariant), and the Coriolis impedance. There may be others, and likely are. Given the spin dependence of the weak interaction, one would expect that adding the longitudinal impedances to the figure would give additional insight into the weak decays, likely essential for instance in impedance-based calculations of those branching ratios.

Present in the plot are several impedances that (excepting the unstable particle spectrum) are absent in our observations of the world, do not couple to the photon, namely those associated with the electric flux quantum, magnetic monopole, and electric dipole. Figure 6 shows this alternation between electric and magnetic with topological complexity.

We see the magnetic flux quantum, electric monopole, and magnetic dipole in the stable particles which comprise our bodies and the air we breathe, but not their electromagnetic complements. It seems that the only place we see these 'dark' components is in the unstable particle spectrum. The origin of this broken symmetry is partially understood in the impedance model[3]. However, its role in the chiral anomaly is not yet obvious.

The impedance approach gives a fresh perspective on anomalies in quantum theory. The chiral anomaly exists in theories of gravity as well. In that case it would seem that there are at least three scale invariant impedances that must be considered - three body, centrifugal, and Coriolis. The question is whether proper consideration of these impedances, whether an impedance approach to gravitation, would be anomaly free as well.

CONCLUSION

Impedances govern the flow of energy. This is a fundamental concept. Historically, it has been overlooked in quantum theory. The first quantum impedance to be discovered, the quantum Hall impedance (an axial vector impedance), was found in 1980, long after the foundations of QED were set in stone and QCD was ascendant.

Despite the remarkable elegance and power of the standard model, proton spin structure remains a mystery[16–19]. The hope is that this preliminary impedance approach to phenomena associated with the chiral anomaly will motivate and illuminate the role of the anomaly in proton spin, and a deeper understanding of spin itself.

ACKNOWLEDGEMENTS

The author thanks Michaele Suisse for discussions, literature searches, and helpful suggestions and comments on drafts of this note, and Michael Creutz for pointing out connections between the impedance model and the chiral anomaly.

* petethepop@aol.com

[1] S. Coon and B. Holstein, "Anomalies in Quantum Mechanics: the $1/r^2$ Potential", Am. J. Phys. 70, 513 (2002). http://arxiv.org/abs/quant-ph/0202091v1

[2] M. Suisse and P. Cameron, "Quantum Interpretation of the Impedance Model", accepted for presentation at the Berlin Conference on Quantum Information and Measurement (March 2014).

[3] P. Cameron, "A Possible Resolution of the Black Hole Information Paradox", Rochester Conferences on Coherence and Quantum Optics and Quantum Information and Measurement (2013), and references therein. http://www.opticsinfobase.org/abstract.cfm?URI=QIM-2013-W6.01

[4] P. Cameron, "Delayed Choice and Weak Measurement in the Nested Mach-Zehnder Interferometer", accepted for presentation at the Berlin Conference on Quantum Information and Measurement (March 2014).

[5] J. Bell and R. Jackiw, "A PCAC Puzzle: $\pi_0 \to \gamma\gamma$ in the σ model", Nuovo Cim. A51, 47 (1969) http://cds.cern.ch/record/348417/files/CM-P00057835.pdf

[6] S. Adler, "Axial vector vertex in spinor electrodynamics", Phys. Rev. 177, 2426 (1969).

[7] R. Jackiw, "Axial Anomaly", Int. J. Mod. Phys. A 25.4 (2010): 659-667. http://hdl.handle.net/1721.1/64480

[8] M. Creutz, "Aspects of chiral symmetry and the lattice" Rev. Mod. Phys., Vol. 73, No. 1, January 2001: 119-150. http://arxiv.org/abs/hep-lat/0007032

[9] Flertcher, N. and Rossing, T., The Physics of Musical Instruments, 2nd ed., Springer, p.19 (1998).

[10] J. Lundeen, "Viewpoint: What Can we Say about a Photon's Past?", Physics 6, 133 (2013). http://physics.aps.org/articles/v6/133

[11] Capps, C., "Near Field or Far Field?", Electronic Design News, p.95 (16 Aug 2001). http://edn.com/design/communications-networking/4340588/Near-field-or-far-field-
Quite remarkably, it is extremely difficult to find a reference for the photon near field impedance in the canonical physics literature, and particularly in the standard grad school electromagnetism textbooks. If you have such a reference, please share it with me.

[12] The mathcad file that generates the impedance plots is available from the author.

[13] MacGregor, M. H., "The Fine-Structure Constant as a Universal Scaling Factor", Lett. Nuovo Cimento 1, p.759-764 (1971).

[14] MacGregor, M. H., "The Electromagnetic Scaling of Particle Lifetimes and Masses", Lett. Nuovo Cimento 31, p.341-346 (1981).

[15] MacGregor, M. H., The Power of Alpha, World Scientific (2007). see also http://70mev.org/alpha/

[16] Krisch, A.D., "Collisions of Spinning Protons", Scientific American, 257, p.42 (1987).

[17] Bass, S., "The Spin Structure of the Proton", Rev.Mod.Phys. 77, p.1257-1302 (2005). http://arxiv.org/abs/hep-ph/0411005

[18] Leader, E., "On the controversy concerning the definition of quark and gluon angular momentum", Phys. Rev. D 83, 096012 (2011). http://arxiv.org/pdf/1101.5956v2.pdf

[19] Aidala, C. et.al., "The Spin Structure of the Nucleon" (2012), Rev.Mod.Phys. 85 (2013) 655-691 http://arxiv.org/abs/1209.2803